2022 American Control Conference (ACC)
Atlanta, USA, June 8-10, 2022

Unified Position-Attitude Control of A Nonlinear Quadrotor Swarm

Boyang Zhang[1] and Henri P. Gavin[1]

Abstract— **In this paper, we propose a novel nonlinear feedback control law to maneuver a swarm of nonlinear quadrotors with interagent collision avoidance. In contrast to the predominant hierarchical control architectures and dynamics linearization in controller synthesis in the literature, we control the position and attitude of each drone simultaneously in one unified step, with no dynamics linearization involved at any stage. Our method is based on generalizations of Gauss's principle of least constraint that allows higher order constrained dynamics and that identifies, stabilizes, and incorporates the time-varying sets of active constraints. The active constraints are asymptotically stabilized to the controlled space according to a generalized constraint stabilization to provide command control actions. Numerical results are provided for a swarm of up to 80 nonlinear quadrotors executing aggressive flights and for eight nonlinear drones swapping positions on a circle, attesting to the efficacy and efficiency of the proposed scheme.**

I. Introduction

Over the past decade, quadrotor swarms have been widely adopted in applications such as inspection and transportation due to their agile and cooperative maneuverability [1]. Due to their nonlinearity, underactuation, and limited battery life, efficient control of a nonlinear quadrotor swarm with collision avoidance remains an open field [2]. According to a recent survey of over 800 papers [3], the majority of methods on quadrotors control employ a hierarchical framework, in which the position and attitude are separately controlled so that the inner loop attitude dynamics is assumed stable and is neglected when designing the outer loop position controller. Such decomposed control of the inherent coupling between quadrotors' translation and rotation may be questionable when subjected to constraint drifts caused by numerical integration errors, unmodeled dynamics, exogenous disturbances, or actuator delays. Moreover, approximately 400 papers adopt linearized quadrotor dynamics that are applied to only small rolls and pitches [3]. This linearization may be void in handling scenarios where aggressive maneuvers are demanded to avoid collisions within a swarm.

Differential flatness based methods [4], [5], [6] derive quadrotors tracking control laws by exploiting four flat outputs (the three-dimensional (3-D) positions of the center of mass and the yaw angle) in a hierarchical framework. In general, these approaches require the knowledge of the reference trajectories of the flat outputs and their derivatives, and angular velocities, to compute control actions that minimize the tracking errors on linear positions and velocities, rotation matrix, and angular velocities. Moreover, collision avoidance is handled by geometric sets [4], by integer constraints [5], or by barrier certificates [6].

To the best of our knowledge, little work has been done on unifying the position and attitude controllers for nonlinear quadrotors. These unified position-attitude control methods include nonlinear model predictive control [7] and sequential linear quadratic control [8]. However, the method in [7] requires the iterative solution of an optimization problem and adopts the small angle assumption for the quadrotor's dynamics, while the approach in [8] involves sequential linearization of the quadrotor dynamics around the trajectory and an iterative solution of a subproblem that has no global optimum guarantee.

In this paper, we propose a unified position-attitude control for a nonlinear quadrotor swarm by noting that a quadrotor's translational and rotational dynamics is fully coupled at the level of snap and angular acceleration. Our method is based on generalizing Gauss's principle of least constraint (GPLC) [9], which is mathematically equivalent to Udwadia-Kalaba (U-K) equations [10]. The GPLC/U-K approaches have been used to analytically describe the constrained dynamics of mechanical systems [11]. However, these methods apply only to second order dynamical systems that are subjected to equality constraints [12].

To our best knowledge, for the first time GPLC is generalized for equality-constrained, higher order dynamical systems and a globally-optimal, nonlinear, unified position-attitude control is developed in [13] for a single nonlinear quadrotor tracking that does not involve any dynamics linearization. In this paper, we extend the work in [13] to control multiple nonlinear quadrotors by introducing inequality constraint and regularization for collision avoidance.

This paper is organized as follows. Section II presents the generalized GPLC control for a general nonlinear dynamical system. Then, a nonlinear unified position-attitude controller is constructed for a nonlinear quadrotor swarm in Section III. Next, Section IV provides numerical results for a multi-quadrotor swarm flight and for eight drones resolving collisions, followed by the contributions and future work in Section V.

II. Constrained Higher Order Systems Control

A. Generalized Gauss's Principle of Least Constraint

1) Second Order Systems: Consider a second order system subject to a set of C equality constraints, $\mathbf{g}(\mathbf{q}, t) = \mathbf{c}$, on the coordinate positions $\mathbf{q} \in \mathbb{R}^{N_q}$, where $\mathbf{c} \in \mathbb{R}^C$ denotes constant thresholds. The constraints on $\mathbf{q}$ require that the

*This work was supported in part by the U.S. Army Research Office under award number 75568-NS-II.

[1]B. Zhang and [1]H.P. Gavin are with Department of Civil and Environmental Engineering, Duke University, Durham, NC, 27708 USA boyang.zhang@duke.edu, henri.gavin@duke.edu.

coordinate accelerations $\ddot{\mathbf{q}}$ satisfy the differential equations

$$\frac{d^2}{dt^2}\mathbf{g}(\mathbf{q},t) = \frac{\partial \mathbf{g}}{\partial \mathbf{q}}\ddot{\mathbf{q}} + \frac{d}{dt}\left(\frac{\partial \mathbf{g}}{\partial \mathbf{q}}\right)\dot{\mathbf{q}} + \frac{d}{dt}\left(\frac{\partial \mathbf{g}}{\partial t}\right) = \mathbf{0} \ , \quad (1)$$

which give rise to a constraint (control) force $\mathbf{f}_\mathrm{c}$. Thus, the dynamics of the controlled system can be expressed by a system of N_q second order ordinary differential equations (ODEs), $\mathbf{M}(\mathbf{q},t)\ddot{\mathbf{q}} = \mathbf{f}(\mathbf{q},\dot{\mathbf{q}},t) = \mathbf{f}_\mathrm{nc} + \mathbf{f}_\mathrm{c}$, where $\mathbf{M}$ is the symmetric positive definite (SPD) mass matrix, and $\mathbf{f}_\mathrm{nc}$ contains all nonconstraint (noncontrol) forces. Equation (1) is linear in $\ddot{\mathbf{q}}$ and may be compactly written as $\mathbf{A}(\mathbf{q},t)\,\ddot{\mathbf{q}} = \mathbf{b}(\mathbf{q},\dot{\mathbf{q}},t)$, where

$$\mathbf{A}(\mathbf{q},t) = \frac{\partial \mathbf{g}}{\partial \mathbf{q}} = \begin{bmatrix} \frac{\partial g_1(\mathbf{q},t)}{\partial q_1} & \cdots & \frac{\partial g_1(\mathbf{q},t)}{\partial q_{N_\mathrm{q}}} \\ \vdots & \ddots & \vdots \\ \frac{\partial g_C(\mathbf{q},t)}{\partial q_1} & \cdots & \frac{\partial g_C(\mathbf{q},t)}{\partial q_{N_\mathrm{q}}} \end{bmatrix} .$$

We note that the unconstrained minimization

$$\min_{\ddot{\mathbf{q}}} \frac{1}{2}\ddot{\mathbf{q}}^\mathsf{T}\mathbf{M}\ddot{\mathbf{q}} - \mathbf{f}_\mathrm{nc}^\mathsf{T}\ddot{\mathbf{q}} \quad (2)$$

is solved by the unconstrained accelerations $\ddot{\mathbf{q}}_\mathrm{u} \triangleq \mathbf{M}^{-1}\mathbf{f}_\mathrm{nc}$, and that imposing (1) to (2) is equivalent to

$$\max_{\boldsymbol{\lambda}} \min_{\ddot{\mathbf{q}}} \frac{1}{2}\ddot{\mathbf{q}}^\mathsf{T}\mathbf{M}\ddot{\mathbf{q}} - \mathbf{f}_\mathrm{nc}^\mathsf{T}\ddot{\mathbf{q}} + \frac{1}{2}\ddot{\mathbf{q}}_\mathrm{u}^\mathsf{T}\mathbf{M}\ddot{\mathbf{q}}_\mathrm{u} + \boldsymbol{\lambda}^\mathsf{T}(\mathbf{A}\ddot{\mathbf{q}} - \mathbf{b}) \ , \quad (3)$$

whose solution is attained by the Karush-Kuhn-Tucker (KKT) conditions

$$\begin{bmatrix} \mathbf{M} & \mathbf{A}^\mathsf{T} \\ \mathbf{A} & \mathbf{0} \end{bmatrix} \begin{bmatrix} \ddot{\mathbf{q}} \\ \boldsymbol{\lambda} \end{bmatrix} = \begin{bmatrix} \mathbf{f}_\mathrm{nc} \\ \mathbf{b} \end{bmatrix} \ , \quad (4)$$

where $\mathbf{0}$ denotes a zero matrix, and $\mathbf{f}_\mathrm{c} \triangleq -\mathbf{A}^\mathsf{T}\boldsymbol{\lambda}$ contains the control actions associated with enforcing (1). Equation (3) is the *original* GPLC (OGPLC) [9], which states that the constrained accelerations $\ddot{\mathbf{q}}$ minimize a quadratic form of the difference between $\ddot{\mathbf{q}}$ and $\ddot{\mathbf{q}}_\mathrm{u}$.

2) Higher Order Systems: The dynamics of a constrained system may involve higher order derivatives of coordinate positions, or it may not be linear in the second order derivatives of coordinate positions but is linear in higher order derivatives.

In this section, we generalize OGPLC and apply it to a controlled higher order system whose dynamics is described by N_q ODEs of various orders, $\mathbf{M}\dot{\mathbf{x}} = \mathbf{f}_\mathrm{nc} + \mathbf{f}_\mathrm{c}$, where each ODE is linear in its highest order derivatives, which are contained in $\dot{\mathbf{x}}$. The vector $\dot{\mathbf{x}}$ can contain derivatives of different orders. $\mathbf{M}$, $\mathbf{f}_\mathrm{nc}$, and $\mathbf{f}_\mathrm{c}$ are respectively the SPD generalized mass matrix, generalized noncontrol forces, and generalized control forces that correspond to the higher order system and cannot involve derivatives included in $\dot{\mathbf{x}}$.

The controlled space for the system is defined based on the equality constraints $\mathbf{g}_\mathrm{eq} = \mathrm{c}_\mathrm{eq}$ and the inequality constraints $\mathbf{g}_\mathrm{in} \leq \mathrm{c}_\mathrm{in}$. Both $\mathbf{g}_\mathrm{eq}$ and $\mathbf{g}_\mathrm{in}$ are functions of the states and the state derivatives up to (but not including) the corresponding orders in $\dot{\mathbf{x}}$. At each time instant, the active constraint set is identified as the collection of all equality constraints and all inequality constraints that exceed their corresponding thresholds. This set of C active constraints is treated as equality constraints $\mathbf{g} = \mathbf{c}$ and varies over time according to the natural evolution of system dynamics. The active constraints may be differentiated κ times with respect to time such that the differentiated form is linear in $\dot{\mathbf{x}}$. By imposing these C linear differential equations $\mathbf{A}\dot{\mathbf{x}} = \mathbf{b}$, the constrained highest order derivatives $\dot{\mathbf{x}}$ solves

$$\max_{\boldsymbol{\lambda}} \min_{\dot{\mathbf{x}}} \frac{1}{2}\dot{\mathbf{x}}^\mathsf{T}\mathbf{M}\dot{\mathbf{x}} - \mathbf{f}_\mathrm{nc}^\mathsf{T}\dot{\mathbf{x}} + \frac{1}{2}\dot{\mathbf{x}}_\mathrm{u}^\mathsf{T}\mathbf{M}\dot{\mathbf{x}}_\mathrm{u} + \boldsymbol{\lambda}^\mathsf{T}(\mathbf{A}\dot{\mathbf{x}} - \mathbf{b}) \ , \quad (5)$$

which we term the *generalized* GPLC (GGPLC), since it assumes an analogous form to that of OGPLC (3). The GGPLC minimizes a quadratic form of the difference between $\dot{\mathbf{x}}$ and the unconstrained highest order derivatives $\dot{\mathbf{x}}_\mathrm{u}$, subjected to differentiated constraints. GGPLC results in a KKT system

$$\begin{bmatrix} \mathbf{M} & \mathbf{A}^\mathsf{T} \\ \mathbf{A} & \mathbf{0} \end{bmatrix} \begin{bmatrix} \dot{\mathbf{x}} \\ \boldsymbol{\lambda} \end{bmatrix} = \begin{bmatrix} \mathbf{f}_\mathrm{nc} \\ \mathbf{b} \end{bmatrix} \ , \quad (6)$$

where $\mathbf{f}_\mathrm{c} \triangleq -\mathbf{A}^\mathsf{T}\boldsymbol{\lambda}$ arises from enforcing the equality constraints $\mathbf{A}\dot{\mathbf{x}} = \mathbf{b}$ and thus may be regarded as command control actions. Hence, Equation (6) represents a nonlinear feedback control law for the higher order dynamical system to obey the constraints at a differentiated level.

Note that in this and the following sections, the variables $\mathbf{M}$, $\mathbf{g}$, $\mathbf{c}$, $\mathbf{A}$, $\mathbf{b}$, $\boldsymbol{\lambda}$, N_q, C, $\mathbf{f}_\mathrm{nc}$, and $\mathbf{f}_\mathrm{c}$ correspond to a system of higher order ODEs, while these variables all correspond to a system of second order ODEs in Section II-A.1.

B. Existence and Uniqueness of the Solution of KKT Systems

Proposition 1: The KKT system (6) is singular if and only if either (a) $\mathbf{A}^\mathsf{T}$ has a nontrivial null space, or (b) the null space of $\mathbf{M}$ intersects the null space of $\mathbf{A}$.

Proof: See Proposition 1 in [13]. ■

C. Generalized Constraint Stabilization

In reality, the imposition of the differentiated constraints

$$\frac{d^\kappa \mathbf{g}}{dt^\kappa} = \mathbf{A}\dot{\mathbf{x}} - \mathbf{b} = \mathbf{0} \quad (7)$$

does not guarantee the satisfaction of the original constraints $\mathbf{g} = \mathbf{c}$ due to constraint drift caused by inconsistent initialization, numerical integration errors, exogenous forces, or unmodeled dynamics. To stabilize constraint dynamics, we enforce asymptotically stable dynamics upon $\mathbf{g}(t)$

$$\frac{d^\kappa \mathbf{g}}{dt^\kappa} + \sum_{i=1}^{\kappa-1} \beta_i \frac{d^i \mathbf{g}}{dt^i} + \beta_0(\mathbf{g} - \mathbf{c}) = \mathbf{0} \ , \quad (8)$$

where β_i are called *Baumgarte coefficients* and are selected to asymptotically stabilize $\mathbf{g}(t)$. Equation (8) is a generalization of Baumgarte's stabilization [12] to higher order constraint dynamics. Substituting (8) into (7), we get

$$\mathbf{A}\dot{\mathbf{x}} = \widehat{\mathbf{b}} \triangleq \mathbf{b} - \sum_{i=1}^{\kappa-1} \beta_i \frac{d^i \mathbf{g}}{dt^i} - \beta_0(\mathbf{g} - \mathbf{c}) \ . \quad (9)$$

For even values of κ, the distinct eigenvalues of (8) can be prescribed in terms of *natural frequencies* ω_i and *damping ratios* ζ_i, $i = 1, \ldots, \kappa/2$, $\sigma_i, \bar{\sigma}_i = -\zeta_i\omega_i + \omega_i\sqrt{\zeta_i^2 - 1}$.

Then, the Baumgarte coefficients of any even order κ can be directly obtained from the companion matrix of (8)

$$\begin{bmatrix} 0 & 1 & 0 & \cdots & 0 \\ 0 & 0 & 1 & \cdots & 0 \\ \vdots & \vdots & & \cdots & \vdots \\ -\beta_0 & -\beta_1 & -\beta_2 & \cdots & -\beta_{\kappa-1} \end{bmatrix} = \mathbf{V}\mathbf{\Lambda}\mathbf{V}^{-1} \ , \quad (10)$$

where $\mathbf{\Lambda}$ is a diagonal matrix of the prescribed eigenvalue pairs, σ_i and $\bar{\sigma}_i$, and the corresponding columns of $\mathbf{V}$ are $[1 \ \sigma_i \ \sigma_i^2 \ \ldots \ \sigma_i^{\kappa-1}]^\mathsf{T}$ and $[1 \ \bar{\sigma}_i \ \bar{\sigma}_i^2 \ \ldots \ \bar{\sigma}_i^{\kappa-1}]^\mathsf{T}$ [14].

Imposing the stabilized constraints (9) instead of (7) in (6), we have

$$\begin{bmatrix} \mathbf{M} & \mathbf{A}^\mathsf{T} \\ \mathbf{A} & \mathbf{0} \end{bmatrix} \begin{bmatrix} \dot{\mathbf{x}} \\ \boldsymbol{\lambda} \end{bmatrix} = \begin{bmatrix} \mathbf{f}_{\mathrm{nc}} \\ \widehat{\mathbf{b}} \end{bmatrix} \ , \quad (11)$$

which we term the GGPLC KKT system with stabilization.

Note that any constraint violation is guaranteed to converge to zero with the dynamics specified by ω_i and ζ_i, since the eigenvalues of (8) are user-prescribed via (10).

D. Regularization

In the following application of GGPLC to control a nonlinear quadrotor swarm with collision avoidance, $\mathbf{A}$ may be a tall matrix under some scenarios, i.e., $C > N_{\mathrm{q}}$. Furthermore, some active constraints may be linearly dependent at some time instants. Hence, the system (11) is regularized so that the regularized KKT matrix is full rank,

$$\begin{bmatrix} \mathbf{M} & \mathbf{A}^\mathsf{T} \\ \mathbf{A} & -\alpha\mathbf{I} \end{bmatrix} \begin{bmatrix} \dot{\mathbf{x}} \\ \boldsymbol{\lambda} \end{bmatrix} = \begin{bmatrix} \mathbf{f}_{\mathrm{nc}} \\ \widehat{\mathbf{b}} \end{bmatrix} \ , \quad (12)$$

where $\mathbf{I}$ is an identity matrix, $0 < \alpha \ll \min\Lambda(\mathbf{M})$ is the regularization factor, where $\min\Lambda(\mathbf{M})$ is the minimum eigenvalue of $\mathbf{M}$, and $\alpha = 0$ yields the original problem (11). The solution of (11) is uniquely approximated by that of (12).

III. Unified Position-Attitude Control for a Constrained nonlinear Quadrotor Swarm

A. Constrained Dynamics

1) A Generic Quadrotor: A quadrotor has six degrees of freedom and four control inputs generated from the four spinning propellers. The inertial frame is fixed to the ground with positive Z axis upwards, while the body frame is fixed at the quadrotor's principle axes with the thrust force acting in the positive body Z axis. In this study, the rotation matrix from the body frame to the inertial frame is parameterized by ZYX Euler angles, roll $\phi \in [-\pi, \pi]$, pitch $\theta \in (-\pi/2, \pi/2)$, and yaw $\psi \in [-\pi, \pi]$,

$$\mathbf{R} \triangleq \begin{bmatrix} \mathbf{x}_\mathrm{B}^\mathsf{T} \\ \mathbf{y}_\mathrm{B}^\mathsf{T} \\ \mathbf{z}_\mathrm{B}^\mathsf{T} \end{bmatrix}^\mathsf{T} = \begin{bmatrix} \mathrm{c}\psi\mathrm{c}\theta & \mathrm{c}\psi\mathrm{s}\theta\mathrm{s}\phi - \mathrm{s}\psi\mathrm{c}\phi & \mathrm{c}\psi\mathrm{s}\theta\mathrm{c}\phi + \mathrm{s}\psi\mathrm{s}\phi \\ \mathrm{s}\psi\mathrm{c}\theta & \mathrm{s}\psi\mathrm{s}\theta\mathrm{s}\phi + \mathrm{c}\psi\mathrm{c}\phi & \mathrm{s}\psi\mathrm{s}\theta\mathrm{c}\phi - \mathrm{c}\psi\mathrm{s}\phi \\ -\mathrm{s}\theta & \mathrm{c}\theta\mathrm{s}\phi & \mathrm{c}\theta\mathrm{c}\phi \end{bmatrix} , \quad (13)$$

where s and c represent sine and cosine, respectively. The Euler angle rates $\dot{\mathbf{\Theta}}_\mathrm{E}$ are calculated by

$$\dot{\mathbf{\Theta}}_\mathrm{E} = \begin{bmatrix} \dot{\phi} \\ \dot{\theta} \\ \dot{\psi} \end{bmatrix} = \mathbf{E}\,\boldsymbol{\omega}_\mathrm{B} = \begin{bmatrix} 1 & \mathrm{s}\phi\,\mathrm{t}\theta & \mathrm{c}\phi\,\mathrm{t}\theta \\ 0 & \mathrm{c}\phi & -\mathrm{s}\phi \\ 0 & \mathrm{s}\phi/\mathrm{c}\theta & \mathrm{c}\phi/\mathrm{c}\theta \end{bmatrix} \boldsymbol{\omega}_\mathrm{B} \, , \quad (14)$$

where t denotes tangent and $\boldsymbol{\omega}_\mathrm{B} = [p \ q \ r]^\mathsf{T} \in \mathbb{R}^3$ are the angular velocities expressed in the body frame.

The quadrotor is assumed to be a rigid body with dynamics formulated by the Newton-Euler equations,

$$m\,\ddot{\mathbf{p}}_\mathrm{I} = f_\mathrm{t}\mathbf{R}\mathbf{e}_3 - mg\,\mathbf{e}_3 = f_\mathrm{t}\mathbf{z}_\mathrm{B} - mg\,\mathbf{e}_3 \ , \quad (15)$$

$$\mathbf{J}\,\dot{\boldsymbol{\omega}}_\mathrm{B} = \boldsymbol{\tau}_\mathbf{B} - \hat{\boldsymbol{\omega}}_\mathrm{B}\mathbf{J}\boldsymbol{\omega}_\mathrm{B} \ , \quad (16)$$

where m is the total mass, g is the gravitational acceleration, $\mathbf{p}_\mathrm{I} = [x \ y \ z]^\mathsf{T}$ are the position coordinates of the center of mass (CoM) expressed in the inertial frame, $\mathbf{e}_3 = [0 \ 0 \ 1]^\mathsf{T}$, f_t is the magnitude of the total thrust force, $\mathbf{J} = \mathrm{diag}(I_x, I_y, I_z)$ is a diagonal matrix of the principal moments of inertia, $\boldsymbol{\tau}_\mathrm{B} = [\tau_1 \ \tau_2 \ \tau_3]^\mathsf{T}$ are the control torques expressed in the body frame, and $\hat{\boldsymbol{\omega}}_\mathrm{B}$ is the skew-symmetric matrix of $\boldsymbol{\omega}_\mathrm{B}$. The inputs in (15) and (16) are f_t and $\boldsymbol{\tau}_\mathrm{B}$, and they can be uniquely determined by the spinning speeds of four propellers [5].

The jerk and snap dynamics in the inertial frame are respectively

$$m\dddot{\mathbf{p}}_\mathrm{I} = \dot{f}_\mathrm{t}\mathbf{z}_\mathrm{B} + f_\mathrm{t}\mathbf{R}\hat{\boldsymbol{\omega}}_\mathrm{B}\mathbf{e}_3 \ , \quad (17)$$

$$m\ddddot{\mathbf{p}}_\mathrm{I} = \ddot{f}_\mathrm{t}\mathbf{z}_\mathrm{B} + 2\dot{f}_\mathrm{t}\mathbf{R}\hat{\boldsymbol{\omega}}_\mathrm{B}\mathbf{e}_3 + f_\mathrm{t}(\mathbf{R}\hat{\boldsymbol{\omega}}_\mathrm{B}^2\mathbf{e}_3 + \mathbf{R}\dot{\hat{\boldsymbol{\omega}}}_\mathrm{B}\mathbf{e}_3) \quad (18)$$

by differentiating (15) and by noting that $\dot{\mathbf{R}} = \mathbf{R}\hat{\boldsymbol{\omega}}_\mathrm{B}$.

Thus, the equations of motion for a nonlinear quadrotor with fully coupled translation and rotation are (18) and (16),

$$\begin{bmatrix} m\mathbf{I}_3 & \mathbf{M}_* \\ \mathbf{0}_{3\times3} & \mathbf{J} \end{bmatrix} \begin{bmatrix} \ddddot{\mathbf{p}}_\mathrm{I} \\ \dot{\boldsymbol{\omega}}_\mathrm{B} \end{bmatrix} = \begin{bmatrix} \ddot{f}_\mathrm{t}\mathbf{z}_\mathrm{B} + 2\dot{f}_\mathrm{t}\mathbf{R}\hat{\boldsymbol{\omega}}_\mathrm{B}\mathbf{e}_3 + f_\mathrm{t}\mathbf{R}\hat{\boldsymbol{\omega}}_\mathrm{B}^2\mathbf{e}_3 \\ \boldsymbol{\tau}_\mathrm{B} - \hat{\boldsymbol{\omega}}_\mathrm{B}\mathbf{J}\boldsymbol{\omega}_\mathrm{B} \end{bmatrix} , \quad (19)$$

where the term

$$\mathbf{M}_*\dot{\boldsymbol{\omega}}_\mathrm{B} \triangleq \begin{bmatrix} f_\mathrm{t}\mathbf{y}_\mathrm{B} & -f_\mathrm{t}\mathbf{x}_\mathrm{B} & \mathbf{0} \end{bmatrix} \begin{bmatrix} \dot{p} & \dot{q} & \dot{r} \end{bmatrix}^\mathsf{T} = -f_\mathrm{t}\mathbf{R}\dot{\hat{\boldsymbol{\omega}}}_\mathrm{B}\mathbf{e}_3$$

achieves the coupling of the rotational dynamics to the translational dynamics according to (18). f_t and $\dot{f}_\mathrm{t}$ are treated as states, and $\ddot{f}_\mathrm{t}$ and $\boldsymbol{\tau}_\mathrm{B}$ are the control inputs that arise when a set of active constraints is associated with the quadrotor.

By noting that the translational and rotational dynamics are fully coupled in (19), we eliminate $\dot{p}$ and $\dot{q}$ by substituting $\dot{p} = [\tau_1 - (I_z - I_y)qr]/I_x$ and $\dot{q} = [\tau_2 - (I_x - I_z)pr]/I_y$ from (16) into (19) to obtain

$$\begin{bmatrix} m\mathbf{I}_3 & \mathbf{0}_{3\times1} \\ \mathbf{0}_{1\times3} & I_z \end{bmatrix} \begin{bmatrix} \ddddot{\mathbf{p}}_\mathrm{I} \\ \dot{r} \end{bmatrix} = \begin{bmatrix} \mathbf{f}_{\mathrm{ut}} \\ (I_x - I_y)pq \end{bmatrix} + \begin{bmatrix} \mathbf{z}_\mathrm{B} & -f_\mathrm{t}\mathbf{y}_\mathrm{B}/I_x & f_\mathrm{t}\mathbf{x}_\mathrm{B}/I_y & \mathbf{0}_{3\times1} \\ 0 & 0 & 0 & 1 \end{bmatrix} \begin{bmatrix} \ddot{f}_\mathrm{t} \\ \boldsymbol{\tau}_\mathrm{B} \end{bmatrix} , \quad (20)$$

where $\mathbf{f}_{\mathrm{ut}} = [(I_y + I_z - I_x)f_\mathrm{t}pr/I_y + 2\dot{f}_\mathrm{t}q]\mathbf{x}_\mathrm{B} + [(I_x + I_z - I_y)f_\mathrm{t}qr/I_x - 2\dot{f}_\mathrm{t}p]\mathbf{y}_\mathrm{B} - [f_\mathrm{t}(p^2 + q^2)]\mathbf{z}_\mathrm{B}$. Note that $\mathbf{x}_\mathrm{B}$, $\mathbf{y}_\mathrm{B}$, and $\mathbf{z}_\mathrm{B}$ are orthonormal column vectors in $\mathbb{R}^3$. As long as the rotors rotate, f_t is nonzero. The remaining coordinates, x, y, z, and r, become fully controllable in a reduced configuration space, with the input influence matrix being full rank. We call the quadrotor model (20) a fourth order system since the highest order in the derivatives $\dot{\mathbf{x}} = [\dddot{\mathbf{p}}_\mathrm{I}^\mathsf{T} \ \ \dot{r}]^\mathsf{T} \in \mathbb{R}^4$ is four.

2) An N-quadrotor Swarm: Equation (20) can be compactly written as $\mathbf{M}_i\dot{\mathbf{x}}_i = \mathbf{f}_{\mathrm{nc}i} + \mathbf{f}_{\mathrm{c}i} \triangleq \mathbf{f}_{\mathrm{nc}i} + \mathbf{B}_i\mathbf{u}_i$ for quadrotor i, $\forall i = 1, \ldots, N$. Hence, the constrained dynamics of an N-quadrotor swarm can be expressed as

$$\mathbf{M}\dot{\mathbf{x}} = \mathbf{f}_{\mathrm{nc}} + \mathbf{f}_{\mathrm{c}} \triangleq \mathbf{f}_{\mathrm{nc}} + \mathbf{B}\mathbf{u} \ , \tag{21}$$

where $\mathbf{M} = \mathrm{diag}(\mathbf{M}_i) \in \mathbb{R}^{4N\times 4N}$ is a block diagonal matrix, $\dot{\mathbf{x}} = [\ldots\ \dot{\mathbf{x}}_i^{\mathsf{T}}\ \ldots]^{\mathsf{T}} \in \mathbb{R}^{4N}$ contains $\dddot{\mathbf{p}}_{\mathrm{I}}$ and $\dot{r}$ for all agents, $\mathbf{B} = \mathrm{diag}(\mathbf{B}_i) \in \mathbb{R}^{4N\times 4N}$ is a block diagonal matrix, and $\mathbf{u} \in \mathbb{R}^{4N}$ contains $\ddot{f}_{\mathrm{t}}$ and $\boldsymbol{\tau}_{\mathrm{B}}$ for all agents.

B. Constraint Formulation

The N-drone swarm may be divided into K subswarms to conduct cooperative tasks. Each subswarm is assigned a guiding virtual leader with position coordinates $\bar{\mathbf{p}}_k(t) = [\bar{x}_k(t)\ \bar{y}_k(t)\ \bar{z}_k(t)]^{\mathsf{T}} \in \mathbb{R}^3$ and has a number of N_k agents, $k = 1, \ldots, K$, such that $\sum_{k=1}^{K} N_k = N$. We define $\mathbf{p} = [\ldots\ \mathbf{p}_i^{\mathsf{T}}\ \ldots]^{\mathsf{T}} \in \mathbb{R}^{3N}$, $\mathbf{p}_i^{\mathsf{T}} = [x_i\ y_i\ z_i] \in \mathbb{R}^3$, $\forall i = 1, \ldots, N$. Each agent is constrained to track its virtual leader $\bar{\mathbf{p}}_k(t)$ along three inertial axes. Mathematically, for agent i this is expressed as three equality constraints

$$\mathbf{g}_{ik} = [g_{ik}^{\mathrm{x}}\ g_{ik}^{\mathrm{y}}\ g_{ik}^{\mathrm{z}}]^{\mathsf{T}} \triangleq \Delta\mathbf{p}_{ik} = \mathbf{p}_i - \bar{\mathbf{p}}_k = \mathbf{0}_{3\times 1} \ , \tag{22}$$

where the superscripts x, y, and z denote the X, Y, and Z coordinate in the inertial frame, respectively.

Furthermore, the agent pair $\{i, j\}$ must prevent collision in 3-D for all neighboring agents during a flight. This is expressed as three inequality constraints

$$\mathbf{g}_{ij} = [g_{ij}^{\mathrm{x}}\ g_{ij}^{\mathrm{y}}\ g_{ij}^{\mathrm{z}}]^{\mathsf{T}} \triangleq |\Delta\mathbf{p}_{ij}| = |\mathbf{p}_i - \mathbf{p}_j| \geq \mathbf{r}_{ij} \ , \tag{23}$$

where $|\cdot|$ denotes absolute value, and the inequality sign denotes componentwise comparison. $\mathbf{g}_{ij}$ are active when the CoM of agents i and j are inside the virtual cuboid with edge lengths $\mathbf{r}_{ij} = [r_{ij}^{\mathrm{x}}\ r_{ij}^{\mathrm{y}}\ r_{ij}^{\mathrm{z}}]^{\mathsf{T}}$, i.e., $|\Delta\mathbf{p}_{ij}| < \mathbf{r}_{ij}$ holds. The constant control parameters $\mathbf{r}_{ij}$ are selected so that the minimum pairwise distance among agents is always greater than the sum of the actual half-lengths of any pair of colliding agents. Note that (23) can be decomposed into an upper and a lower branch

$$\mathbf{g}_{ij}^{\mathrm{u}} = [g_{ij}^{\mathrm{xu}}\ g_{ij}^{\mathrm{yu}}\ g_{ij}^{\mathrm{zu}}]^{\mathsf{T}} \triangleq \Delta\mathbf{p}_{ij} \leq -\mathbf{r}_{ij} \ , \tag{24}$$

$$\mathbf{g}_{ij}^{\mathrm{l}} = [g_{ij}^{\mathrm{xl}}\ g_{ij}^{\mathrm{yl}}\ g_{ij}^{\mathrm{zl}}]^{\mathsf{T}} \triangleq \Delta\mathbf{p}_{ji} \leq -\mathbf{r}_{ij} \ , \tag{25}$$

where the superscripts u and l denote upper and lower, respectively.

C. Constraint Stabilization

Whether the trio of the inequality constraints, $g_{ij}^{\mathrm{x}} \in [g_{ij}^{\mathrm{xu}}\ g_{ij}^{\mathrm{xl}}]$, $g_{ij}^{\mathrm{y}} \in [g_{ij}^{\mathrm{yu}}\ g_{ij}^{\mathrm{yl}}]$, and $g_{ij}^{\mathrm{z}} \in [g_{ij}^{\mathrm{zu}}\ g_{ij}^{\mathrm{zl}}]$, is included in or excluded from the active constraint set is determined by comparing the relative distances $|\Delta\mathbf{p}_{ij}|$ to their corresponding thresholds $\mathbf{r}_{ij}$ componentwise at each time step. This time-varying set of active inequality constraints along with the equality tracking constraints is differentiated as (7), stabilized as (9), and incorporated into (12) to give rise to GGPLC controls. Hence, the active constraints can be stabilized as

$$\begin{aligned}
\ddddot{\mathbf{g}}_{ik} &= -\beta_3^{\mathrm{t}}\dddot{\mathbf{g}}_{ik} - \beta_2^{\mathrm{t}}\ddot{\mathbf{g}}_{ik} - \beta_1^{\mathrm{t}}\dot{\mathbf{g}}_{ik} - \beta_0^{\mathrm{t}}\mathbf{g}_{ik} \triangleq \widehat{\mathbf{b}}_{ik}^{\mathrm{t}} \ , \\
\dddot{\mathbf{g}}_{ij}^{\mathrm{u}} &= -\beta_3^{\mathrm{c}}\ddot{\mathbf{g}}_{ij}^{\mathrm{u}} - \beta_2^{\mathrm{c}}\dot{\mathbf{g}}_{ij}^{\mathrm{u}} - \beta_1^{\mathrm{c}}\mathbf{g}_{ij}^{\mathrm{u}} - \beta_0^{\mathrm{c}}(\Delta\mathbf{p}_{ij} + \mathbf{r}_{ij}) \triangleq \widehat{\mathbf{b}}_{ij}^{\mathrm{cu}} \ , \\
\dddot{\mathbf{g}}_{ij}^{\mathrm{l}} &= \beta_3^{\mathrm{c}}\ddot{\mathbf{g}}_{ij}^{\mathrm{u}} + \beta_2^{\mathrm{c}}\dot{\mathbf{g}}_{ij}^{\mathrm{u}} + \beta_1^{\mathrm{c}}\mathbf{g}_{ij}^{\mathrm{u}} + \beta_0^{\mathrm{c}}(\Delta\mathbf{p}_{ij} - \mathbf{r}_{ij}) \triangleq \widehat{\mathbf{b}}_{ij}^{\mathrm{cl}} \ ,
\end{aligned} \tag{26}$$

where the superscripts t and c respectively denote tracking and collision.

D. Selection of Baumgarte Coefficients

The Baumgarte coefficients β_i^{t} and β_i^{c}, $i = 0, 1, 2, 3$, in the fourth order constraint dynamics (26) are control parameters in this unified position-attitude controller for a nonlinear quadrotor swarm. During the natural evolution of constrained system dynamics, the onset of an active constraint g leads to initial conditions $g_{\mathrm{in}} = c$ (c is the threshold of the constraint) and generically nonzero (problem dependent) $\dot{g}_{\mathrm{in}}$, $\ddot{g}_{\mathrm{in}}$, and $\dddot{g}_{\mathrm{in}}$, with higher order dynamics having a generally higher initial value. Thus, an optimization problem that minimizes the peak constraint position over time subject to nonzero initial constraint conditions can be posed to find an optimal set of Baumgarte coefficients,

$$\begin{aligned}
&\min_{\omega_i,\zeta_i} \max_{t}\ g(\mathbf{q}, t) \qquad g_{\mathrm{in}} = c,\ \dot{g}_{\mathrm{in}} = 1,\ \ddot{g}_{\mathrm{in}} = 2,\ \dddot{g}_{\mathrm{in}} = 3 \\
&\text{s.t. } |\omega_i|_{\min} \leq |\omega_i| \leq |\omega_i|_{\max} \quad \text{and} \quad \zeta_{i,\min} \leq \zeta_i \leq \zeta_{i,\max}
\end{aligned} \tag{27}$$

where the natural frequencies and damping ratios of the constraint dynamics are prescribed to lie within user-specified ranges.

E. Regularized GGPLC KKT System with Stabilization

Equation (12) describes a nonlinear quadrotor swarm by substituting constrained system dynamics (21) and constraint dynamics (26) into (12). From (26), the generic row of $\mathbf{A}$ for $\mathbf{g}_{ik}$ is $[\mathbf{0}\ 1\ \mathbf{0}]$, with the entry 1 on column $4i-3$, $4i-2$, and $4i-1$ for g_{ik}^{x}, g_{ik}^{y}, g_{ik}^{z}, respectively. The generic row of $\mathbf{A}$ corresponding to $\mathbf{g}_{ij}^{\mathrm{u}}$ is $[\mathbf{0}\ 1\ \mathbf{0}\ -1\ \mathbf{0}]$, with the entry 1 on column $4i-3$, $4i-2$, $4i-1$ and -1 on column $4j-3$, $4j-2$, $4j-1$ for g_{ij}^{xu}, g_{ij}^{yu}, g_{ij}^{zu}, respectively. The row of $\mathbf{A}$ for $\mathbf{g}_{ij}^{\mathrm{l}}$ is the opposite of the corresponding row for $\mathbf{g}_{ij}^{\mathrm{u}}$.

Upon solving the matrix equation (12) at each time instant, we associate $-\mathbf{A}^{\mathsf{T}}\boldsymbol{\lambda}$ with $\mathbf{B}\mathbf{u}$ in (21) to provide the controls for all agents that enforce tracking and collision avoidance along three inertial axes. Note that $\mathbf{B}$ is full rank in all scenarios except for any drone with a zero f_{t}. Hence, the command control actions for all agents can be obtained by $\mathbf{u} = -\mathbf{B}^{-1}\mathbf{A}^{\mathsf{T}}\boldsymbol{\lambda}$. Then, $\dot{p}$ and $\dot{q}$ for each drone can be obtained by substituting the corresponding τ_1 and τ_2 in $\mathbf{u}$ into (16). The actual inputs to a quadrotor generated by the four propellers are (equivalently) f_{t} and $\boldsymbol{\tau}_{\mathrm{B}}$, where f_{t} is a state in the GGPLC control and is equal to double integrating $\ddot{f}_{\mathrm{t}}$ in $\mathbf{u}$.

The constant-step fourth order Runge–Kutta method is used for numerical integration, where each drone has 20 states: $\mathbf{p}_{\mathrm{I}}$, $\dot{\mathbf{p}}_{\mathrm{I}}$, $\ddot{\mathbf{p}}_{\mathrm{I}}$, $\dddot{\mathbf{p}}_{\mathrm{I}}$, $\boldsymbol{\Theta}_{\mathrm{E}}$, $\boldsymbol{\omega}_{\mathrm{B}}$, f_{t}, and $\dot{f}_{\mathrm{t}}$.

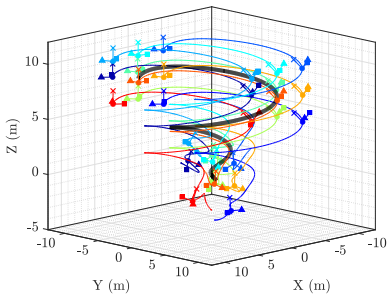

Fig. 1: 10 quadrotors track a virtual leader (black solid line) with three snapshots ($t = 2, 9, 16$ s) of the drones' body frames. The square ■, triangle ▲, and cross × heads denote the positive body X, Y, and Z axes, respectively. Each drone executes a sufficiently smooth path (a colored solid line) that results from reacting purely to its constrained nonlinear dynamics. All agents execute smooth motions and coordinate their motions with their neighbors and the virtual leader after the initial stage. The corresponding animation can be found online. [1]

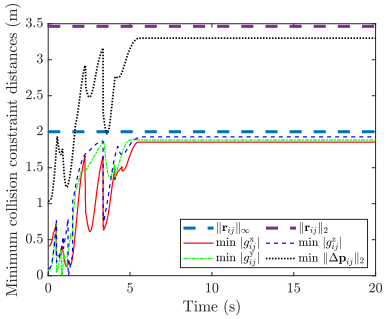

Fig. 2: Minimum relative distances and its components along the three inertial axes for all quadrotor pairs with active trio of collision avoidance constraints. Such minimum relative distances along different directions are stabilized closer to the corresponding thresholds.

IV. Numerical Examples

The proposed GGPLC control for multiple nonlinear quadrotors is verified by performing numerical simulations with a constant time step $\Delta t = 0.005$ s in MATLAB on a Windows desktop with a 2.50-GHz Intel Xeon E5-2680v3 CPU.

1) Single Swarming: In this example, we simulate a swarm of homogeneous nonlinear quadrotors. The parameters used are: $m = 5$ kg, $g = 9.8$ m/s^2, $2I_x = 2I_y = I_z = 1$ kg·m^2, $\alpha = m/10^4$. The control parameters take the values $\beta_0^{\mathrm{t}} = 97.409$, $\beta_1^{\mathrm{t}} = 125.02$, $\beta_2^{\mathrm{t}} = 59.851$, $\beta_3^{\mathrm{t}} = 12.667$, $\beta_0^{\mathrm{c}} = 1558.5$, $\beta_1^{\mathrm{c}} = 982.3$, $\beta_2^{\mathrm{c}} = 233.73$, $\beta_3^{\mathrm{c}} = 24.882$, the number of virtual leader is $k = 1$, and $\mathbf{r}_{ij} = \mathbf{2}_{3\times 1}$. Fig. 1 illustrates the trajectories of 10 nonlinear quadrotors guided by a conical spiral virtual leader moving from $(0, 0, 0)$ to $(2.5, -8.5, 8)$ for $t \in [0, 12]$ s, during which the reference's first through fourth order time derivatives vary smoothly from zero to zero. The virtual leader stays stationary at $(2.5, -8.5, 8)$ for $t > 12$ s. Each drone has all zero initial states except the initial thrust $f_{\mathrm{t}} = mg$ and the initial position randomly drawn within a cube centered at the origin with edges parallel to the axes and with an edge length of 7.

The snapshots of all drones' body frames at $t = 2$, 9, and 16 s are also shown in Fig. 1. At the initial 5 s, all drones react to the constrained quadrotor swarm dynamics in a dynamic and nonuniform manner (snapshot at $t = 2$ s as a representative illustration), as seen from the first 5 seconds in Fig. 2. Due to the enforced constraint stabilization, the minimum relative distances over all active colliding drone pairs asymptotically converge to the thresholds of the controlled space. For $t \in (5, 12]$ s, the swarm is self organized into an equilibrium shape with all agents' motions synchronized (snapshot at $t = 9$ s as a representative illustration), where the thrust axis (positive body Z axis) of each drone tilts inwards the spiral at large roll and pitch angles, overcoming the gravity and the centrifugal force. This stable swarm flight stage ($t \in (5, 12]$ s) can also be evidenced from stabilized minimum relative distances in Fig. 2. When the reference

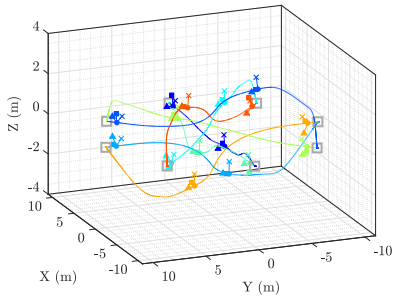

Fig. 3: 8 drones swap equally spaced positions (gray squares) on a circle of radius 10 m on the X-Y plane ($z = 0$) with two snapshots ($t = 0.4, 3$ s) of the drones' body frames. The markers ■, ▲, and × denote the positive body X, Y, and Z axes, respectively. Each drone executes a sufficiently smooth path (a colored solid line) that results from reacting purely to its constrained nonlinear dynamics. The corresponding animation is available online. [2]

is at rest after $t = 12$ s, all drones remain horizontal hover (snapshot at $t = 16$ s as a representative illustration) with control thrusts counterbalancing gravity and with zero control torques.

2) Swapping Positions: In this example, the control parameters are chosen as $\beta_0^{\mathrm{t}} = 492.9803$, $\beta_1^{\mathrm{t}} = 999.0483$, $\beta_2^{\mathrm{t}} = 399.5673$, $\beta_3^{\mathrm{t}} = 44.9958$, $\beta_0^{\mathrm{c}} = 97.409$, $\beta_1^{\mathrm{c}} = 117.49$, $\beta_2^{\mathrm{c}} = 55.057$, $\beta_3^{\mathrm{c}} = 11.904$, the number of virtual leader is $k = 8$, and $\mathbf{r}_{ij} = \mathbf{6}_{3\times 1}$. Fig. 3 depicts eight nonlinear quadrotors swapping equally spaced positions on a circle of radius 10 m located on the X-Y plane ($z = 0$). Each drone is associated with a virtual leader which remains stationary at the agent's goal position for all time. At the initial 0.5 s, all drones are accelerating by having positive body Z axes pointing towards their goals (snapshot at $t = 0.4$ s as a representative illustration). For $t \in (0.5, 5.4]$ s, the quadrotors negotiate trajectories by reacting purely to the constrained swarm dynamics (snapshot at $t = 3$ s as a representative illustration). For $t \in (5.4, 11]$ s, all agents converge to their goals due only to the tracking control actions, as no collision avoidance constraints are active from Fig. 4. Then, all drones are stabilized at their goal positions in horizontal hover for $t \in (11, 20]$ s, as evidenced from the stabilized body thrust forces that counterbalance the gravity in Fig. 5.

[1] https://youtu.be/ChReGTNtA_g

[2] https://youtu.be/JX-al2Lx3dM

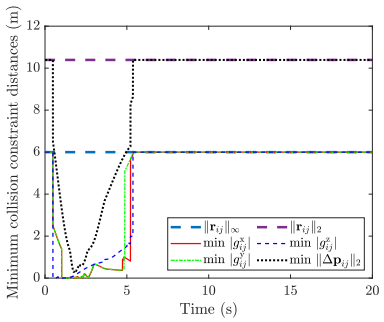

Fig. 4: Minimum relative distances and its components along the three inertial axes for all quadrotor pairs with active trio of collision avoidance constraints. Such minimum relative distances along different directions are stabilized closer to the corresponding thresholds.

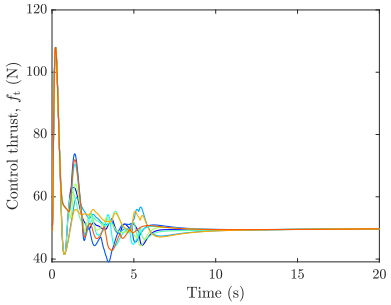

Fig. 5: Total thrust magnitude of 8 drones expressed in the body frame.

TABLE I: COMPUTATION TIME PER ITERATION (MILLISECONDS) FOR A SWARM OF N NONLINEAR MINIATURE QUADROTORS

N	5	10	20	40	80
t (ms)	0.0653	0.0690	0.0968	0.250	0.602

3) Computational Efficiency: Table I presents the elapsed real time for obtaining control actions for different numbers of agents for single swarm tracking as in Section IV-.1. m, I_x, I_y, I_z, α, and $\mathbf{r}_{ij}$ are all scaled to one fifth of those used in Section IV-.1, resulting in a much crowded configuration and thus more active constraints. The only differences in the simulation setup between these runs are the number of agents and the uniformly generated random initial positions for all agents. The computation time counts the time accumulated over the simulation span to identify active set of constraints, to construct every term in (12), and to solve for the command control actions $\mathbf{u}$ and the highest order derivatives $\dot{\mathbf{x}}$. Then, the computation time per iteration is calculated by dividing the total elapsed time by the total number of numerical integration steps. Similarly, the computation time per iteration for the case study in Section IV-.2 is 6.134×10^{-5} s. Table I demonstrates that the proposed control law is computationally efficient for a swarm of up to at least 80 nonlinear quadrotors.

V. CONTRIBUTIONS AND FUTURE WORK

We have proposed an efficient, novel, nonlinear feedback control law for general constrained systems and applied it to simultaneously control the positions and attitudes of multiple nonlinear quadrotors subjected to 3-D tracking and collision avoidance constraints. Our method is based on a generalization of Gauss's principle of least constraint (GPLC) combined with a generalized constraint stabilization. At each time instant, the active constraints are dynamically identified, differentiated, stabilized, and incorporated to compute nonlinear feedback controls that drive nonlinear system dynamics to obey constraints by simply solving a KKT system (a linear matrix equation) without iteration.

To the best of our knowledge, this work is (a) the first generalization of GPLC to control a *general* (in terms of constraint type and system dynamics order) constrained dynamical system, and (b) the first *true* nonlinear unified position-attitude control of a quadrotor swarm with collision avoidance by exploiting nonlinear quadrotor dynamics with a solution uniqueness guarantee. Note that no linearization or iteration is involved at any stage in our framework.

Along this promising line of research, the proposed control can be further developed to investigate its performance subject to obstacle avoidance, actuator delay, modeling uncertainties, exogenous disturbances, sensor noise, and decentralized architectures. Furthermore, the proposed method is amenable to physical validations thanks to its computational efficiency.

REFERENCES

[1] S.-J. Chung, A. A. Paranjape, P. Dames, S. Shen, and V. Kumar, "A survey on aerial swarm robotics," *IEEE Trans. Robot.*, vol. 34, no. 4, pp. 837–855, 2018.

[2] S. Huang, R. S. H. Teo, and K. K. Tan, "Collision avoidance of multi unmanned aerial vehicles: A review," *Annu. Rev. Contr.*, vol. 48, pp. 147–164, 2019.

[3] T. P. Nascimento and M. Saska, "Position and attitude control of multi-rotor aerial vehicles: A survey," *Annu. Rev. Contr.*, vol. 48, pp. 129–146, 2019.

[4] J. H. Gillula, G. M. Hoffmann, H. Huang, M. P. Vitus, and C. J. Tomlin, "Applications of hybrid reachability analysis to robotic aerial vehicles," *Int. J. Robot. Res.*, vol. 30, no. 3, pp. 335–354, 2011.

[5] D. Mellinger, A. Kushleyev, and V. Kumar, "Mixed-integer quadratic program trajectory generation for heterogeneous quadrotor teams," in *Proc. IEEE Int. Conf. Robot. Autom.*, 2012, pp. 477–483.

[6] L. Wang, A. D. Ames, and M. Egerstedt, "Safe certificate-based maneuvers for teams of quadrotors using differential flatness," in *Proc. IEEE Int. Conf. Robot. Autom.*, 2017, pp. 3293–3298.

[7] A. Murilo and R. V. Lopes, "Unified NMPC framework for attitude and position control for a VTOL UAV," *Proc. Inst. Mech. Eng. I*, vol. 233, no. 7, pp. 889–903, 2019.

[8] C. De Crousaz, F. Farshidian, M. Neunert, and J. Buchli, "Unified motion control for dynamic quadrotor maneuvers demonstrated on slung load and rotor failure tasks," in *Proc. IEEE Int. Conf. Robot. Autom.*, 2015, pp. 2223–2229.

[9] C. F. Gauß, "Über ein neues allgemeines grundgesetz der mechanik." *J. für die Reine und Angew. Math.*, vol. 4, pp. 232–235, 1829.

[10] F. E. Udwadia and R. E. Kalaba, "A new perspective on constrained motion," *Proc.: Math. Phys. Sci.*, vol. 439, no. 1906, pp. 407–410, 1992.

[11] B. Shirani, M. Najafi, and I. Izadi, "Cooperative load transportation using multiple UAVs," *Aerosp. Sci. Technol.*, vol. 84, pp. 158–169, 2019.

[12] B. Zhang and H. P. Gavin, "Gauss's principle with inequality constraints for multiagent navigation and control," *IEEE Trans. Automat. Contr.*, vol. 67, no. 2, pp. 810–823, 2022.

[13] B. Zhang and H. P. Gavin, "Unified position and attitude control of a fully nonlinear quadrotor," in *Proc. Am. Control Conf.*, 2021, pp. 1064–1069.

[14] D. S. Bernstein, *Matrix Mathematics: Theory, Facts, and Formulas*, 2nd ed. Princeton, NJ, USA: Princeton University Press, 2009.